HHS Public Access

Author manuscript

Atmos Pollut Res. Author manuscript; available in PMC 2021 September 01.

Published in final edited form as:

Atmos Pollut Res. 2020 September ; 11(9): 1481–1486. doi:10.1016/j.apr.2020.05.026.

Electron microscopic characterization of exhaust particles containing lead dibromide beads expelled from aircraft burning leaded gasoline

Jack D. Griffith[a]

[a]Lineberger Comprehensive Cancer Center, Departments of Microbiology and Immunology, And Biochemistry and Biophysics University of North Carolina at Chapel Hill, Chapel Hill, NC, 27955, USA

Abstract

Piston powered aircraft burning leaded gasoline contribute ~70% of the lead in the atmosphere in the US. The physical size, composition, and structure of aircraft exhaust particles containing lead dibromide are poorly understood and heretofore have not been examined directly by electron microscopy (EM), in particular when captured from an aircraft in flight. To accomplish this, exhaust samples were trapped on EM supports within 10–15 ms of exiting the aircraft exhaust pipe. High angle annular detector dark field scanning EM revealed irregular particles with a mean diameter of 13 nm consisting of a 4 nm microcrystal of lead dibromide surrounded by a halo of hydrocarbons. In contrast, exhaust particles from an automobile burning leaded fuel averaged 35 nm in diameter and contained 5–10, 4 nm lead beads. Of significant concern, the smaller aircraft particles could penetrate mucosal barriers in the lung and be readily taken up by epithelial cells.

Keywords

Aircraft exhaust; Electron microscopy; HAADF/STEM; Lead dibromide; Air pollution; Lung mucosa; Lung cancer

1. Introduction

Nanoscale particles containing lead dibromide are expelled in the exhaust of piston powered aircraft burning leaded gasoline. Lead additives were eliminated by the mid 1990's in motor vehicle fuels, reducing the atmospheric lead levels by > 98%. However, leaded gasoline continues to be used in piston powered general aviation (GA) aircraft and contributed 70% (458 tons in 2017) of the lead present in the atmosphere in the US with the remainder derived mainly from industrial processes (U.S. EPA, 2009; U.S. EPA, 2017). Relatively little is known about the physical size, composition, and structure of lead-containing particles

jdg@med.unc.edu.

Author statement

As a single author paper, this author developed the study, collected the data and wrote the paper. The author also flew the aircraft used in the study.

Declaration of competing interest

The author declares he has no actual or potential competing financial interests.

expelled in aircraft exhaust and this presents a major impediment in understanding their biological impact, in particular on young children. Inhalation of particles containing lead constitutes a serious health risk. In young children lead is taken up in the developing brain via calcium pathways leading to learning and developmental deficits (Canfield et al., 2003; Chiodo et al., 2004; Miranda et al 2007, 2010; Nriagu, 1990; Schnaas et al., 2006). Indeed studies have suggested that the reduction in IQ levels in children exposed to lead from aviation gasoline emissions may constitute a 1 billion dollar a year economic loss in the US (Wolfe et al., 2016; Zahran et al., 2017).

Tetraethyl lead compounds were developed in the 1930's to reduce pre-detonation in motor vehicles engines that can lead to engine failure. This allowed development of more powerful higher octane fuels. While modern automobile engines operate on unleaded gasoline, the transition to unleaded fuel in piston powered aircraft engines has not been achieved due to the required high power output of these engines. Aviation fuel, termed 100 LL (100 octane, low lead), still contains ~2 g of lead per gallon (Royal Dutch Shell, 2010). In contrast, turboprops and jets burn kerosene (Jet-A) which does not contain lead. Lead deposits foul engines unless scavenged following combustion. This is accomplished by including organohalides in the gasoline, which react with the volatilized lead to form lead halides and are expelled as nanoscale particles containing lead-dibromide.

Levels of atmospheric lead resulting from motor vehicle emissions peaked in the mid 1970's reaching 0.1–1 μg of lead/m^3 in large US cities, hundreds of times higher than background levels of 0.0006 μg/m^3 (U.S. EPA, 2013). Of particular concern, measurement of blood lead levels in children in metropolitan areas were often in the range of 10–30 μg per dL. Blood lead levels of 100 μg/dL can lead to death and neurological impairment. In children where a significant amount of lead is taken up in the developing brain, it has been argued that neurological deficits may be detected at blood lead levels as low as 2 μg/dL (Canfield et al., 2003; Chiodo et al., 2004; Miranda et al 2007, 2010; Schnaas et al., 2006). (In adults 95% of the lead is deposited in bone at equilibrium). Following transition to unleaded gasoline, atmospheric lead levels dropped greatly and blood lead levels in children decreased in parallel with 1–3 μg/dL being typical (summarized in Nriagu, 1990). However, IQ deficits have been observed at blood lead levels near the detection limit (Canfield et al., 2003; Chiodo et al., 2004; Miranda et al 2007, 2010; Schnaas et al., 2006) and the EPA has stated that there is no safe level of lead for children.

Recent studies (Ostro et al., 2015) emphasized the increased risk for brain cancer and other diseases resulting from inhalation of nanoscale particles of a variety of composition. Particle size is critical in determining the effectiveness at which they can penetrate the lung defenses. Button, Kesimer and colleagues (Button et al., 2012; Kesimer et al., 2013) examined the ability of nanoparticles 5–40 nm or greater in diameter to penetrate the cell-surface attached mucins of the periciliary region or the glycocalyx that lines the airways to gain access to epithelial cells. Nanoparticles 40 nm in diameter were excluded while ones 18 nm or smaller passed through and penetrated to the cells. This difference may be a key factor influencing blood lead levels. Previous work showed that the size of lead particles from automotive exhaust ranges from ~20 nm to 100 nm averaging around 50 nm (Little and Wiffen, 1977; reviewed in Xue et al., 2015).

There are reasons to believe that particles containing lead from aircraft exhaust might be significantly smaller than those from motor vehicles. In automobiles, exhaust gasses are restricted as they cool and pass through the exhaust system providing time for lead dibromide particles to coalesce with the exhaust hydrocarbons. In contrast, in piston powered aircraft engines, the exhaust leaves the cylinders ~1300 °F and moves through a much shorter exhaust system. As the hot gasses exit the exhaust pipe they collide with the 100 to 250 mph air-stream, which could generate significant shear forces that might reduce the size of exhaust aggregates. However the shearing forces are likely to be much less important than the short length of the aircraft exhaust system and the high temperature of the exiting gasses. These factors are even greater in large twin-engine aircraft where the engines are often turbocharged, expel the gasses at a higher temperatures, burn significantly more fuel per hour, and fly faster and at higher altitudes. Indeed this class of GA aircraft consumes the major amount of 100 LL fuel in the US each year. The absence of any direct imaging of exhaust particles, in particular ones collected from aircraft in flight prompted us to carry out the work described here, along with a comparison of particles from the exhaust of a vintage automobile engine built to operate on leaded fuel.

2. Materials and Methods

2.1. Preparation of EM supports

Thin carbon foils were prepared by evaporating pure carbon onto freshly cleaved mica sheets in a high vacuum. The carbon foil was floated off onto the surface of hot (70–90 °C) distilled water in a Petri dish and 400 mesh copper or nickel grids (Pella Inc) were placed on the floating film and allowed to remain for 12 h. The grids were lifted from the surface and prior to use treated with a glow discharge for 3 min at a vacuum of 300 torr to place charges on their surface and render them hydrophilic.

2.2. Collection of aircraft exhaust particles

The aircraft used for this study was a 1959 Piper Super Cub with a normally carbureted 160 hp 4 cylinder Lycoming 0–320 engine (Fig. 1A and B). The airplane was operated on 100 LL fuel. Collection tubes were constructed from 50 ml plastic tubes by drilling holes in the bottom to allow air flow and packing the tubes loosely with glass wool (Fig. 1C). From 4 to 6 carbon covered 400 mesh EM grids were placed in or on top of the glass wool and the tubes capped prior to use. For collection, 3 to 4 tubes were attached to the landing struts of the airplane directly in line with the exhaust gasses and 2 feet from the end of the exhaust pipe (Fig. 1B). The tubes were capped until just before takeoff followed by flight at a normal rpm (2400 rpm). The tubes were immediately capped after landing and the EM grids stored in a closed box until examination.

2.3. Collection of automobile exhaust particles

The automobile engine used for this study was in a 1957 Ford Thunderbird (312 cubic inch V-8 and 4 barrel Holey carburetor). The engine was run on unleaded gasoline for 15–20 min to reach normal operating temperature, and the fuel source then switched to 100 LL aviation gasoline. Tailed EM grids were glued by the tails of the grids to wooden sticks and placed 2

feet from the end of the exhaust pipe while the engine ran at 1500–2000 rpm for 15 min. The grids were then removed and placed in a closed box until examination.

2.4. Electron microscopy

The EM grids were examined in a FEI T12 TEM/STEM at 40 kV in the TEM mode and images were collected using a Gatan Orius 4 K × 4 K CCD camera operating with Gatan DM4 Digital Micrograph software. This software was used for measurement of particle dimensions. The grids were also examined in a FEI ThermoFisher Talos TEM/STEM instrument at 200 kV in direct TEM modes or HAADF/STEM imaging and also using an EDS collector in the STEM mode. Images were collected using a CETA 4 K × 4 K digital camera. The images were converted to jpeg format and measurements made with Image J software. Image contrast was adjusted with Adobe Photoshop and arranged into panels for publication. In the enlarged panel in Fig. 6B the micron bar was copied and moved into the region that was cropped from the original full image.

3. Results

To directly image particles expelled in the exhaust of a piston powered aircraft in flight using 100 LL gasoline 50 ml plastic tubes were loosely filled with glass wool, and EM supports placed in or on top of the glass wool. The tubes were attached to the outside of a Piper Super Cub (Fig. 1 A-C), (Materials and Methods). From the 100-mph aircraft speed and the distance between the exhaust pipe and collecting tube, it can be estimated that the exhaust particles could have been trapped on the EM supports within 10–15 ms of exiting the exhaust pipe. Four flights of 30–60 min were carried out and a total of 16 collection tubes were used. Over 50 different EM grids were examined and the results were highly consistent with minor and expected variations depending on the length of the flight and location of the collection tubes relative to the exhaust flow. No differences were observed in the nature of the exhaust particles or their size distribution between grids lying on top of the glass wool and those embedded within the glass wool. However grids placed on top of the wool cushion were often lost due to the air currents. For comparison, a 1957 Ford Thunderbird automobile built to operate on leaded fuel was run on 100LL gasoline. Once the V-8 engine had attained normal operating temperature, the EM grids were glued by their tails to wooden sticks and placed 2 feet from the exhaust port (Materials and Methods). Three collections averaging 15 min each were carried out on separate days and the 20 EM grids examined showed very similar consistent results.

EM grids from the automotive exhaust collections were examined by transmission electron microscopy (TEM) at 40 kV without contrast enhancement since lead is extremely electron dense while hydrocarbon material is much less so. Fields of distinct irregularly shaped particles were observed (Fig. 2A) consisting of numerous tiny electron-dense beads embedded within masses of less electron dense material presumably consisting of a complex of hydrocarbon products. Measurement (n = 86) of the size of the exhaust particles showed a range from 10 to nearly 100 nm with a mean of 35 nm (Fig. 3A), in good agreement with previous studies (Little and Wiffen, 1977; reviewed in Xue et al., 2015). The mean number

of lead beads per particle was 5.4 (n = 86) and the size of the individual lead beads ranged from 2 to 5 nm with a mean of 4 nm (n = 93) (Fig. 3B).

The bulk of the total mass lay in the larger particles (35 nm or greater) and for these, the number of beads per particle was at least 10. The background also included similar irregular, relatively electron transparent masses that did not contain lead beads. Occasionally, larger, apparently solid lead particles ranging from 10 to 30 nm, were observed. However, as shown below, they mostly consisted of closely packed bundles of 4 nm beads. Fields of material deposited on the EM supports from the aircraft exhaust imaged in the TEM mode, were much smaller in size (Fig. 2B). The same 4 nm lead beads were present embedded within similar relatively electron transparent material. Most however, contained only one lead bead. Larger lead particles were also observed at a low frequency.

To obtain higher resolution, the grids from the aircraft collections were examined in a 200 kV TEM/STEM instrument equipped with a high angle annular dark field detector (HAADF/STEM) (Materials and Methods). This modality of dark field imaging is particularly sensitive to high molecular weight elements and, thus, ideally suited to this study. The images (Fig. 2C and D) revealed fields similar to those seen in the TEM mode, but with higher resolution and greater definition of the lead beads and hydrocarbon shell. Larger lead particles were occasionally present (Fig. 2C). The mean size of the exhaust particles including the hydrocarbon shell was 13 nm (n = 239), with a range from 7 to 20 nm (Fig. 3A), several fold smaller than the automotive particles, and most contained only 1 lead bead (mean of 1.2 per particle, n = 227). The small lead beads had a mean diameter of 4 nm (n = 232), the same as seen in the automotive collection (Fig. 3B).

EDS/STEM imaging of a field of particles for lead or bromine (Fig. 4 A-C) showed an abundant amount of each element at the location of two large particles in the field supporting their lead dibromide composition. EDS spectra of fields of particles from both the aircraft and automotive exhaust showed identical results. In the spectra, prominent X-ray lines were present, resulting from lead, bromine (which overlaps with aluminum), carbon, and, either copper or nickel depending on which metal was used for the EM grids (Fig. 5).

HAADF/STEM imaging of individual lead beads in the particles from the automotive exhaust (Fig. 6A and B) revealed the presence of crystal lattices with spacings of 4.7 Å. A 4.7 Å spacing for crystals of lead dibromide crystals had been reported (Ren et al., 1997) further confirming their nature.

4. Discussion

This study represents the first EM visualization of exhaust particles emitted from a piston powered aircraft in flight burning leaded fuel. The transit time from the exhaust port to the EM grids was as short as 10–15 ms and imaging was done without any contrast enhancement other than that provided by the EM itself. The aircraft exhaust particles consist of very small (13 nm on average) masses of hydrocarbon combustion products usually containing only a single lead dibromide microcrystal bead. In contrast, exhaust particles from the automobile engine measured 20–100 nm with a mean diameter of 35 nm and

contained 5–10 lead dibromide beads. A study (Rindlisbacher, 2007) of the exhaust composition from an 0–320 Lycoming engine running on 100LL gasoline (the same type of engine used here) revealed that in addition to carbon soot, and gasses (NO, CO, CO_2), that a complex mixture of C1- > C8 carbonyl products are generated with formaldehyde (C1), a known carcinogen, accounting for over half the total hydrocarbons.

Any sampling procedure will introduce some bias. The observation that there was no detectible difference in particle size distribution between the EM grids placed on the top of the glass wool (aircraft collection) and the grids embedded deeper in the glass wool inside the collection tubes argues that the wool itself did not lead to any selective loss of particles. The 10–15 ms between the exhaust particles exiting the exhaust pipe and impinging on the EM grids was likely so short that little selective loss of small or large particles would have occurred. Since the EM grids did not undergo any treatments prior to imaging (shadow-casting, staining, washing) selective losses resulting from such steps often used in other EM studies were not relevant here. However rare very large lead particles might have been overlooked in examining the EM grids.

The EPA has estimated that 16 million people in the US live within 1 km of an airport in which aircraft using leaded fuel operate, including 3 million children (U.S. EPA, 2010). Miranda and colleagues (Miranda et al., 2011) investigated the blood lead levels of children living in proximity of several airports in North Carolina and found a small but measurable (4%) increase in blood lead levels for children living in close proximity to the airports relative to children living more distantly. As IQ deficits have been detected at the lower limit of blood lead level measurements, this small increase has potential significance. Carr and colleagues (Carr et al., 2011) carried out an analysis of atmospheric lead in the proximity of an airport with high levels of GA piston powered aircraft operations and provided a modeling of the lead concentrations at different sites at the airport. In 2008, criteria for the safe level of atmospheric lead was lowered from 1.5 $\mu g/m^3$ to 0.15 $\mu g/m^3$. Based on this current value, Carr et al. identified hot spots exceeding 0.15 $\mu g/m^3$ in the run-up and take off areas of the airport, with lead levels dropping off in proportion to the distance from the hot spots and airport, in general. However, if in the future, the safe atmospheric lead level will be further reduced to below 0.15 $\mu g/m^3$, then a far greater region of unsafe atmospheric lead levels would be seen to surround these and most other airports and this would include a much larger number of people.

The International Agency for Research on Cancer (IARC) classified inorganic Pb compounds as probable human carcinogens. As shown here, for the particles containing lead expelled in aircraft exhaust this is confounded by their extremely small size. It can be estimated that per gram of lead placed in the atmosphere from aircraft there would be at least 5 times more particles generated relative to legacy emissions from motor vehicles, and due to their very small size, the aircraft generated particles would remain in the air for longer times. Depending on meteorological factors (wind, rain, local geography) these microscopic lead-containing particles might build up over airports for considerable time before being swept away by strong winds or rain. Whether a single particle 20–100 nm in size containing 5–10 lead dibromide beads is more toxic to cells than a ~13 nm one containing a single lead di-bromide bead is unclear. The demonstration (Button et al 2012;

Kesimer et al 2013) that 18 nm particles readily penetrate the mucosal barriers and gain direct access to the lung epithelial cells points to their higher toxicity. This also depends on the charge the particles carry and, further, as the hydrocarbon shell is likely hydrophobic, this would cause the particles to bind to the o-linked glycans. The 4 nm lead beads may then be released and enter the epithelial cells. These observations raise significant questions for further studies. Specifically how tightly are the 4 nm lead dibromide beads bound to the hydrocarbon matrix and how toxic, itself, is the hydrocarbon matrix itself in which they are imbedded?

5. Conclusions

As a result of these studies we conclude that: 1) exhaust emissions from piston powered aircraft burning leaded fuel consist of usually single 4 nm lead dibromide microcrystal beads embedded in a matrix of burned hydrocarbons; 2) the size distribution of the aircraft exhaust particles (13 nm mean diameter) is several fold smaller than the size distribution of exhaust particles from legacy automobiles burning the same leaded fuel; 3) while the exhaust particles from a motor vehicle burning leaded fuel are larger, the particles contain 5–10 of the 4 nm lead dibromide beads.

Acknowledgements

I wish to thank Ray Wassel, James Bonner, Ilona Jaspers, Brian Button and Mehmet Kesimer for helpful discussion. The author thanks Nirwan Tandukar for measurement of the particle sizes on the EM images and their analysis. Amar Shankar Kumbhar in the CHANL facility at UNC-Chapel Hill helped with the imaging in the 200 kV Talos TEM/STEM. This work was funded in part by a grant from the National Institutes of Environmental Health Sciences (R56 E031773).

References

Zahran S, Iverson T, McElmurry SP, Weiler S, 2017 The effect of leaded aviation gasoline on blood lead in children. Assoc. Env. Res. Econ. (JAERE) 4 (2), 575–610.

Button B, Cai L-H, Ehre C, Kesimer M, Hill DB, Sheehan JK, Boucher RC, Rubinstein M, 2012 Periciliary brush promotes the lung health by separating the mucus layer from airway epithelia. Science 337 (6097), 937–941. [PubMed: 22923574]

Canfield RL, Henderson CR, Cory-Slechta DA, Cox C, Jusko TA, Lanphear BP, 2003 Intellectual impairment in children with blood lead concentrations below 10 micro gm per deciliter. N. Engl. J. Med 348, 1517–1526. [PubMed: 12700371]

Carr E, Lee M, Marin K, Holder C, Hoyer M, Pedde M, Cook R, Touma J, 2011 Development and evaluation of an air quality modeling approach to assess near-field impacts of lead emissions from piston-engine aircraft operating on leaded aviation gasoline. Atmos. Environ 45, 5795–5804.

Chiodo LM, Jacobson SW, Jacobson JL, 2004 Neurodevelopmental effects of postnatal lead exposure at very low levels. Neurotoxicol. Teratol 26, 359–371. [PubMed: 15113598]

Kesimer M, Ehre C, Burns KA, Davis CW, Sheehan JK, Pickles RJ, 2013 Molecular organization of the mucins and glycocalyx underlying mucus transport over mucosal surfaces of the airways. Mucosal Immunol. 6 (2), 379–392. [PubMed: 22929560]

Little P, Wiffen RD, 1977 Emission and deposition of lead from motor exhausts II. Airborne concentration, particle size and deposition of lead near motorways. Atmos. Environ 12, 1331–1341 1977.

Miranda ML, Kim D, Galeano MA, Paul JC, Hull AP, Morgan SP, 2007 The relationship between early childhood blood lead levels and performance on End of Grade Tests. Environ. Health Perspect 115, 1242–1247. [PubMed: 17687454]

Miranda ML, Maxson P, Kim D, 2010 Early childhood lead exposure and exceptionality designations for students. Int J Child Health Hum Dev 3 (1), 77–84. [PubMed: 21533004]

Miranda ML, Anthopolos R, Hastings D, 2011 A geospatial analysis of the effects of aviation gasoline on childhood blood lead levels. Environ. Health Perspect 119 (10), 1513–1516. 10.1289/ehp.1003231. [PubMed: 21749964]

Nriagu JO, 1990 The rise and fall of leaded gasoline. Sci. Total Environ 92, 13–28.

Ostro B, Hu J, Goldberg D, Reynolds P, Hertz A, Bernstein L, Kleeman MJ, 2015 Associations of mortality with long-term exposures to fine and ultrafine particles, species and sources: results from the California teachers study cohort. Environ. Health Perspect 123 (6), 549–556. [PubMed: 25633926]

Ren Q, Ding L-Y, Chen F-S, Cheng R-P, Xu D, 1997 The optical properties of lead bromide crystals. J. Mater. Sci. Lett 16, 1247–1248 1997.

Rindlisbacher T, 2007 Aircraft Piston Engine Emissions, Summary Report. 33-05- 003 Piston Engine Emissions Swiss FOCA Summary Report 070612.

Royal Dutch Shell, 2010 Avgas grades and specifications. Available: http://www.shell.com/home/content/aviation/products/fuels/types/avgas/, Accessed date: 15 February 2011.

Schnaas L, Rothenberg SJ, Flores MF, Martinez S, Hernandez C, Osorio E, Velasco SR, Perroni E, 2006 Reduced intellectual development in children with prenatal lead exposure. Environ. Health Perspect 114, 791–797. [PubMed: 16675439]

U.S. EPA (U.S. Environmental Protection Agency), 2009 Electronic report on the environment. Available at: http://cfpub.epa.gov/roe.

U.S. EPA (U.S. Environmental Protection Agency), 2010 Advance notice of proposed rulemaking on lead emissions from piston-engine aircraft using leaded aviation gasoline. Fed. Regist 75, 22440–22468.

TheU.S. EPA (Environmental Protection Agency), 2017 National emissions inventory is available. https://www.epa.gov/air-emissions-inventories/2017-national-emissions-inventory-nei-data.

Wolfe PJ, Giang A, Ashok A, Selin NE, Barrett SRH, 2016 Costs of IQ loss from leaded aviation gasoline emissions. Environ. Sci. Technol 5017 9026–903.

Xue J, Wang X, Durbin TD, Johnson KC, Karavalakis G, Asa-Awuku A, Villela M, Quiros D, Hu S, Huai T, Ayala A, Jung A(, 2015 Comparison of vehicle exhaust particle szie distributions measured by SMPS and EEPS during steady-state conditions. Aerolsol Science and Technology 49 (10), 984–996. 10.1080/02786826.2015.1088146.

Fig. 1.

Sample collection for aircraft exhaust particles. (A). Aircraft used in the study, arrows point to the location of the collecting tube (B). (C) 50 ml tube with glass wool and EM supports (arrows).

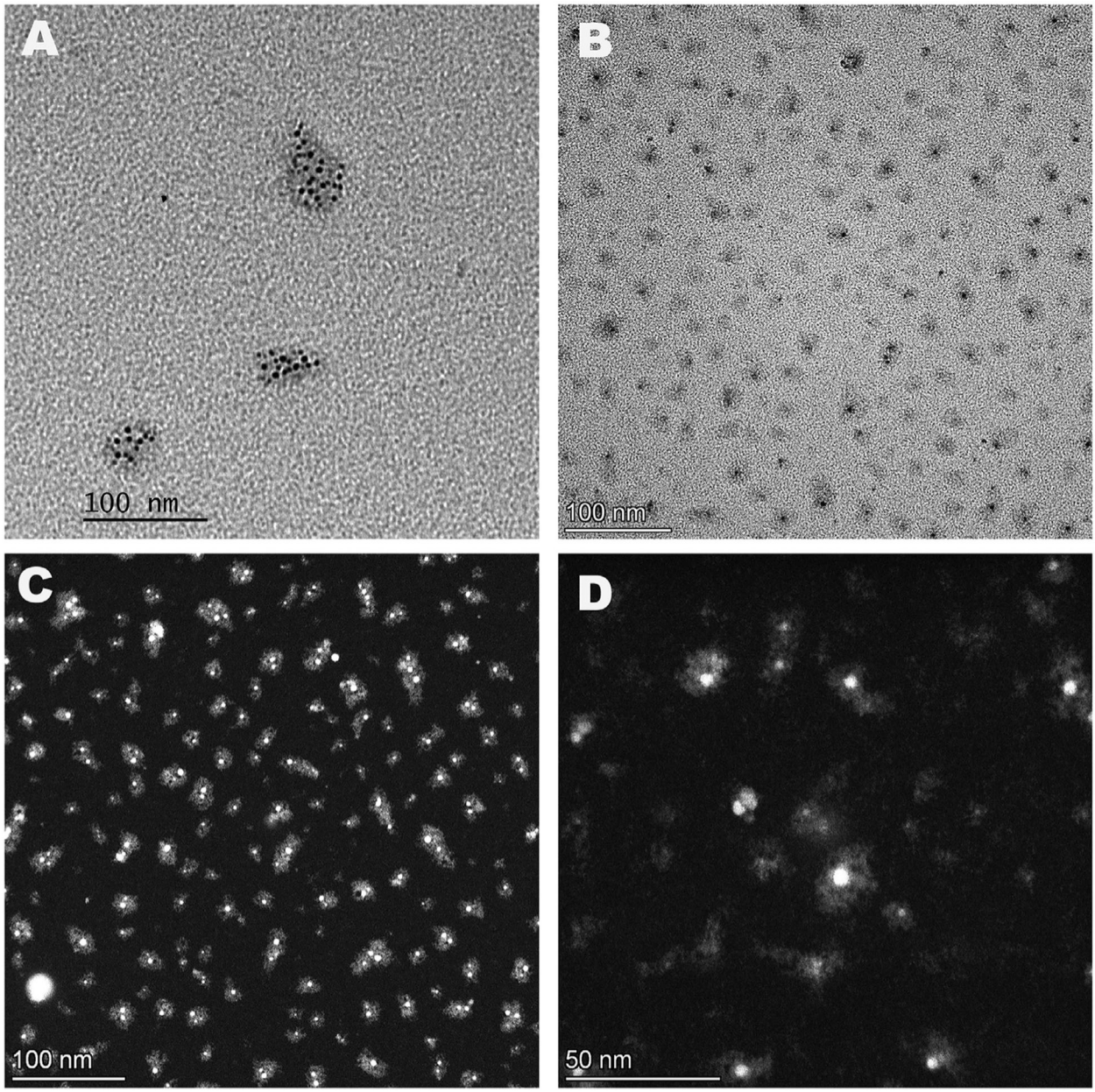

Fig. 2.

TEM and HAADF imaging of exhaust particles containing lead di-bromide. (A). TEM image (40 kV) of exhaust particles from motor vehicle exhaust. (B) TEM image of exhaust particles form aircraft exhaust, same magnification in A and B. (C, D) HAADF dark field images (200 kV STEM) of exhaust particles from aircraft exhaust.

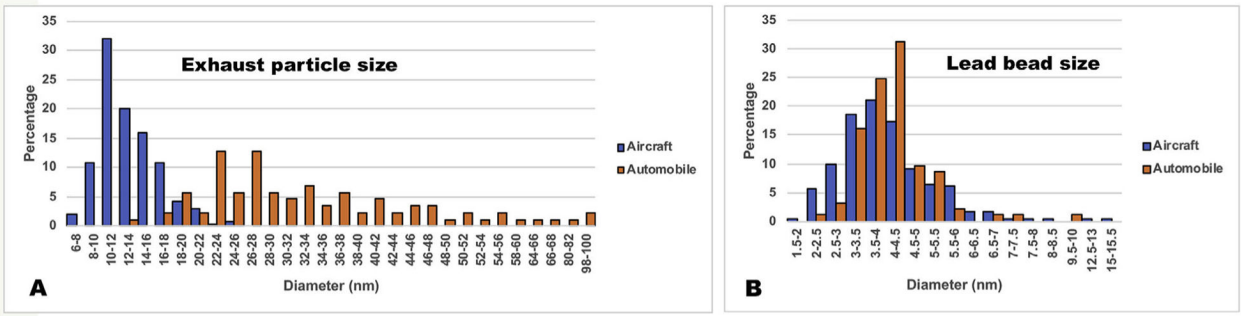

Fig. 3.

Particle sizes for aircraft and motor vehicle exhaust particles. (A). Distribution of particle sizes for aircraft (blue) and motor vehicle (orange) measured as the diameter of the particle including the hydrocarbon shell. (B) Distribution of the sizes of the lead di-bromide beads present in the exhaust particles from the aircraft (blue) and motor vehicle (orange).

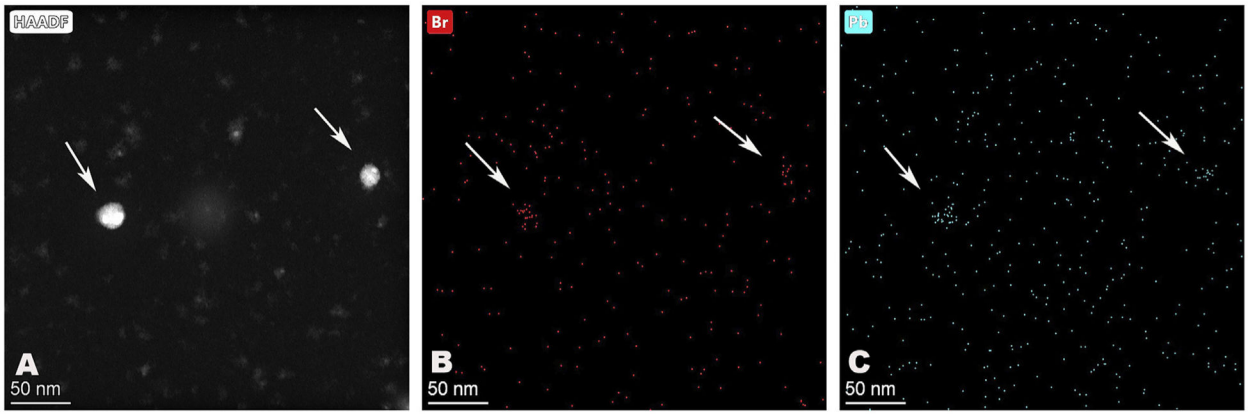

Fig. 4.

HAADF/STEM images of a field of lead di-bromide particles from a motor vehicle exhaust. (A). HAADF/STEM image. (B) Image filtered for bromine. (C) Image filtered for lead. Arrows point to two larger exhaust particles.

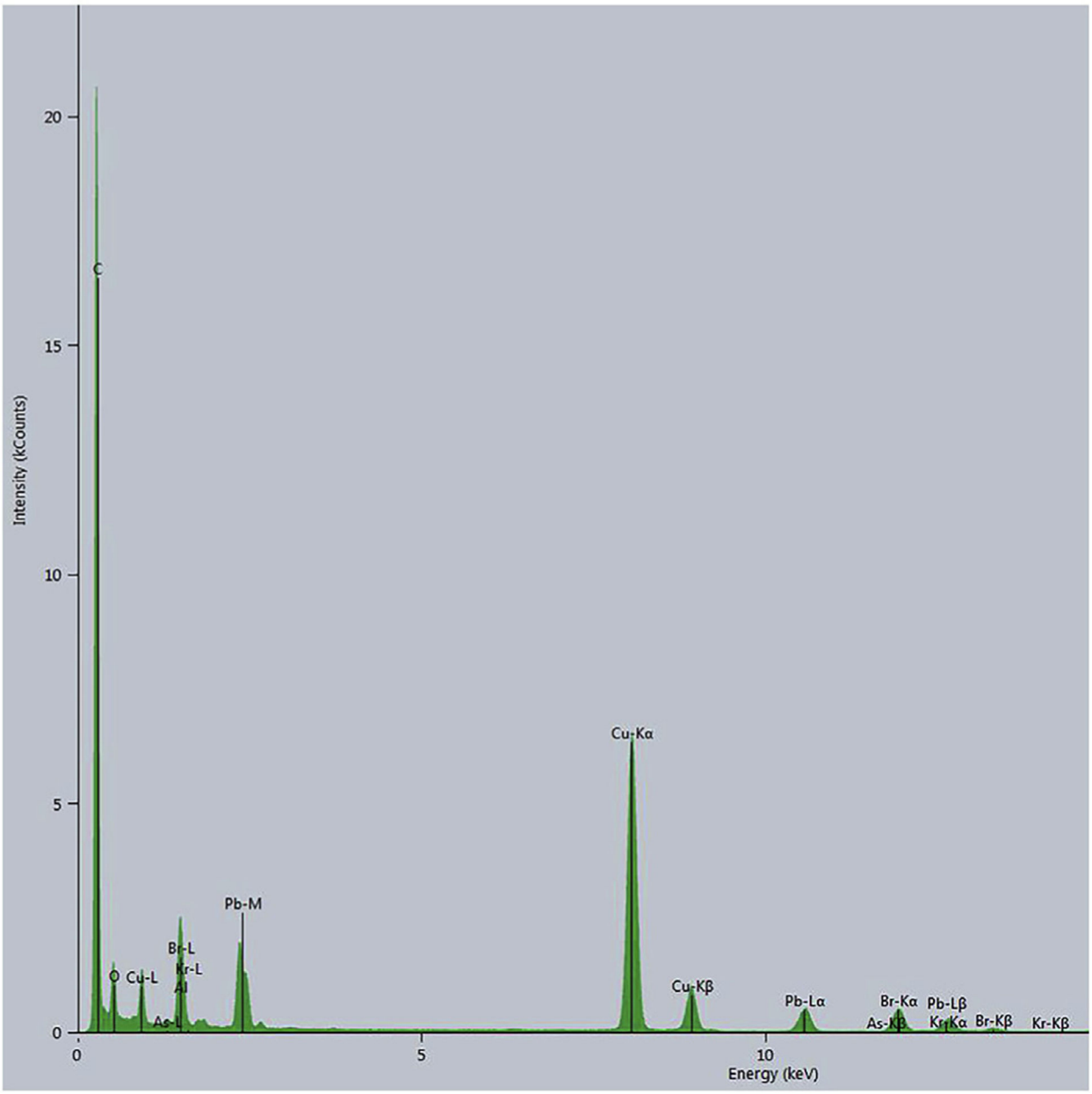

Fig. 5.

EDX spectra of a field of lead di-bromide exhaust particles. A field of exhaust particles from the aircraft exhaust was imaged by HAADF/STEM and then an EDX spectrum taken. Peaks for lead, bromine are prominent. Copper peak reflects the copper supporting grid as this peak is replaced with a nickel peak if nickel grids are employed.

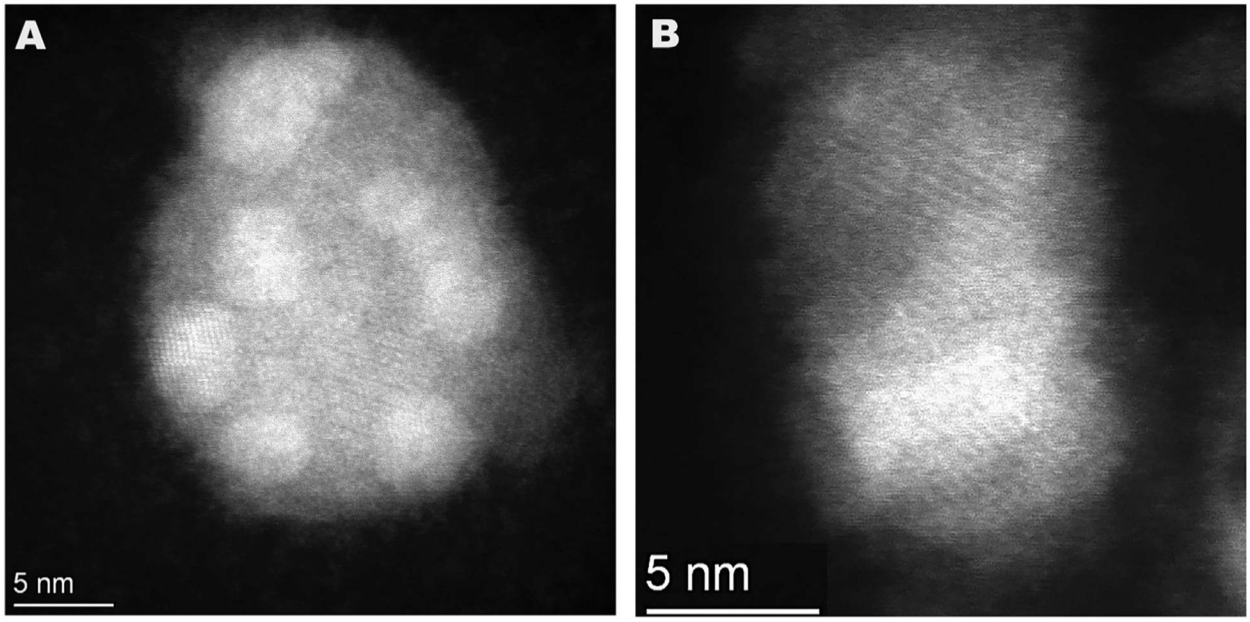

Fig. 6.

High magnification HAADF/STEM images of lead di-bromide particles from motor vehicle exhaust. (A). A single large exhaust particle from the motor vehicle exhaust collection is seen to be composed of many small lead di-bromide microcrystal beads. (B) higher magnification reveals a 4.7 Å lattice diagnostic of lead di-bromide crystals.